Rare charm decays at LHCb

O. Kochebina

PROCEEDINGS OF SCIENCE

Rare charm decays at LHCb

Olga KOCHEBINA*

Université de Paris-Sud 11, Laboratoire de l'Accélérateur Linéaire, CNRS/IN2P3, France
†

E-mail: olga.kochebina@cern.ch

Flavour-changing neutral current decays such as $c \to ul^+l^-$ are highly suppressed in the Standard Model, but may be enhanced by New Physics. The latest searches for such decays at LHCb based on 1.0 fb^{-1} of data collected in 2011 are presented in this document. Two decays, 2-body $D^0 \to \mu^+\mu^-$ and 3-body $D^+_{(s)} \to \pi^+\mu^+\mu^-$, are considered here.

The European Physical Society Conference on High Energy Physics
18-24 July, 2013
Stockholm, Sweden

*Speaker.
†on behalf of the LHCb Collaboration

PoS(EPS-HEP 2013)355

1. Introduction

Rare charm decays proceed mostly through the $c \to u$ Flavor Changing Neutral Current (FCNC), which is possible only at loop diagram level in the Standard Model (SM). Moreover, for rare charm decays, unlike for B decays, there is not a very massive particle, such as the top quark, which can enter the loop diagram to mitigate the GIM suppression. Consequently, rare charm decays are good tools to probe to New Physics (NP) beyond the SM. NP particles can contribute in the loop diagrams and become detectable by causing observables such as branching ratios and CP-, T-odd and angular asymmetries to deviate from the SM predictions [1, 2, 3]. The LHCb searches benefit of large $c\bar{c}$ production cross section [4], which is ~ 20 times higher than the $b\bar{b}$ production cross section.

The LHCb detector [5] is a single-arm forward spectrometer covering the pseudorapidity range $2 < \eta < 5$, designed for the study of particles containing b or c quarks. The detector includes a high precision tracking system consisting of a silicon-strip vertex detector surrounding the pp interaction region, a large-area silicon-strip detector located upstream of a dipole magnet with a bending power of about 4 Tm, and three stations of silicon-strip detectors and straw drift tubes placed downstream. The combined tracking system has a momentum resolution $\Delta p/p$ that varies from 0.4% at 5GeV/c to 0.6% at 100GeV/c, and an impact parameter resolution of 20 μm for tracks with high transverse momentum. Charged hadrons are identified using two ring-imaging Cherenkov detectors. Photon, electron and hadron candidates are identified by a calorimeter system consisting of scintillating-pad and preshower detectors, an electromagnetic calorimeter and a hadronic calorimeter. Muons are identified by a system composed of alternating layers of iron and multiwire proportional chambers. The LHCb trigger system [6] consists of a hardware stage, based on information from the calorimeter and muon systems, followed by a software stage which applies a full event reconstruction.

2. General analysis strategy

Rare charm searches make use of the highly flexible and configurable software trigger that divides the available bandwidth among many specific *lines*. A series of such lines, similar to offline selections, were designed to ensure a high trigger efficiency for rare charm decays and their control modes. These control modes are used to determine the performance with which signal decays are reconstructed, identified, selected and triggered on. This constitutes a first step in the analyses presented in this document.

The detection of very rare decays requires the rejection of combinatorial background to be particularly performant. For that purpose offline selections are based on typical kinematical and topological properties of the signal decays. This comprises the transverse momenta of the particles involved in the decay and quantities that indicate the presence of a long lived particle emerging from the primary vertex and decaying at a displaced vertex. The analyses presented in this document maximise the power of these quantities to distinguish signal from background by using boosted decision trees.

Normalized measurements are performed to minimize systematic uncertainties and prevent having to use the $c\bar{c}$ cross section measurements, which would yield an important additional un-

certainties. Normalization modes are decays that have a similar final state as the signal and are consequently reconstructed and selected with similar efficiency. The branching fractions (BF) of the studied decays is measured by using the known branching fraction of the normalization mode: $BF_{signal} = BF_{norm} \times \frac{\varepsilon_{norm}}{\varepsilon_{signal}} \times \frac{N_{signal}}{N_{norm}}$, where N_{signal}, N_{norm} are the signal and normalization yields, and where ε_{signal}, ε_{norm} are the efficiencies with which they are reconstructed, selected and triggered on.

Efficiencies are calculated using Monte Carlo simulation, corrected with the help of control samples selected in real data. A large part of the systematic effects cancels in the efficiency ratio, yielding corrections typically of a few per cent.

The searches presented in this document are based on blind analyses. Upper limits on branching fractions are derived using the CLs method [7].

3. Recent results on rare charm decays at LHCb with 2011 data

In this section resent results on searches at LHCb of two rare charm channels are presented, namely the 2-body decay $D^0 \to \mu^+\mu^-$ and 3-body FCNC decays $D^+_{(s)} \to \pi^+\mu^+\mu^-$ and lepton number violating (LNV) $D^+_{(s)} \to \pi^-\mu^+\mu^+$ decays. The results presented here were obtained using a dataset corresponding to an integrated luminosity of 1.0 fb^{-1} collected in 2011 at $\sqrt{s} = 7$ TeV.

Charm meson hadronic decays to two, three or four charged hadrons occur at the percent level. This is more than six orders of magnitude higher than the signal and therefore constitutes and important source of additional backgrounds that peak in the invariant mass region close to the signal mass peak, when two of the hadrons in the final state are misidentified as muons. To reduce the rate at which pions are misidentified as muons, a likelihood combining the information from the muon system, the calorimeter and the RICH detectors are applied.

3.1 Search for $D^0 \to \mu^+\mu^-$

According to the SM, this mode is extremely suppressed ($BF(D^0 \to \mu^+\mu^-) < 6 \times 10^{-11}$ [8]). Nevertheless some NP models, like MSSM-RPV where FCNC are possible at the tree level, predict that the BF could be as high as $\sim 10^{-9}$ [9]. The best upper limit before 2012 was published by the Belle collaboration, $BF(D^0 \to \mu^+\mu^-) < 1.4 \times 10^{-7}$ @ 90% *CL* [10].

The LHCb analysis is performed using $D^{*+} \to D^0(\mu^+\mu^-)\pi^+$ decays, with the D^{*+} produced directly at the pp collision primary vertex. The searches are done in the two-dimensional distribution of invariant mass $m(D^0)$ versus invariant mass difference $\Delta m = m(D^{*+}) - m(D^0)$ (see Figure 1). The signal is confined within a very narrow peak in the distribution of the second variable with an excellent resolution (typically 0.3 MeV/c^2). It is therefore a powerful variable to control the backgrounds. The resolution is particularly good thanks to a kinematical fit forcing the π^+ to come from the primary vertex.

$D^0 \to \pi^+\pi^-$ is used as a normalization mode. This final state has different trigger and PID criteria compared to the signal. This calls for special care in the determination of the corresponding efficiencies since the systematic errors associated with these efficiencies do not cancel. The efficiency determination is based on real data, namely on the $D^0 \to K^-\pi^+$ and $J/\psi \to \mu^+\mu^-$ control modes.

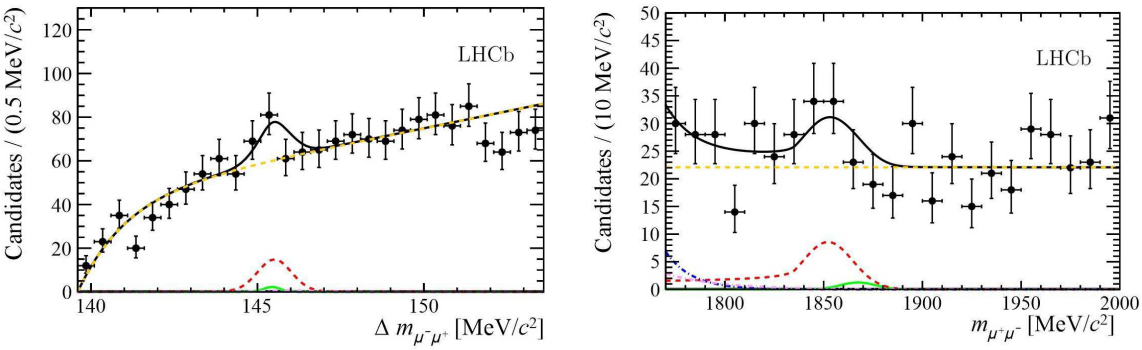

Figure 1: Invariant mass difference $\Delta m = m(D^{*+}) - m(D^0)$ (on the left) and invariant mass $m(D^0)$ (on the right) for $D^{*+} \to D^0(\mu^+\mu^-)\pi^+$ candidates. The projections of the two-dimensional fit are overlaid. The curves represent the total distribution (solid black), the $D^{*+} \to D^0(\pi^+\pi^-)\pi^+$ (dashed red), the combinatorial background (dashed orange), the $D^{*+} \to D^0(K^-\pi^+)\pi^+$ (dash-dotted blue), the $D^{*+} \to D^0(\pi^-\mu^+\nu_\mu)\pi^+$ (dash-dotted purple) and the signal $D^{*+} \to D^0(\mu^+\mu^-)\pi^+$ (solid green) contributions.

One of the corner stones in LHCb's analysis [11], is the use of tight muon identification criteria. It is possible thanks to a precise determination of LHCb's performance in terms of pion to muon misidentification. We used real data with a high statistics control mode $D^0 \to K^-\pi^+$.

The obtained upper limit is $BF(D^0 \to \mu^+\mu^-) < 7.6 \times 10^{-9}$ @ 95% *CL* [11].

3.2 Search for $D^+_{(s)} \to \pi^+\mu^+\mu^-$ and $D^+_{(s)} \to \pi^-\mu^+\mu^+$

The SM short distance contributions to $D^+_{(s)} \to \pi^+\mu^+\mu^-$ are FCNCs that add up to $\sim 10^{-11} - 10^{-9}$ [12]. This could be enhanced according some models beyond the SM up to measurable level [2, 3, 13]. The same final state can be reached via intermediate resonances η, ρ, ω and ϕ decaying to $\mu^+\mu^-$. These long distance contributions have BF of the order 10^{-6} and could overwhelm any enhancement from NP. Therefore experimental searches are performed in regions of dimuon mass away from resonances.

The most stringent limits published so far are $BF(D^+ \to \pi^+\mu^+\mu^-) < 3.9 \times 10^{-6}$ (90% CL) [14] and $BF(D^+_s \to \pi^+\mu^+\mu^-) < 2.6 \times 10^{-5}$ (90% CL) [15].

The LHCb analysis uses $D^+ \to \pi^+\phi(\mu^+\mu^-)$ as a normalization mode. Its final state is identical to that of the signal, therefore a better cancellation of systematics uncertainties is expected. This decay is also used as a signal proxy to optimize the selection and define the shape of the PDF fitted to the data.

The yield of the $D^+ \to \pi^+\pi^+\pi^-$ peaking background is measured by the same fit that determines the signal yield. To help the fitter, the shape of this background is determined using another sample, where the muon identification cuts have been loosened in order to obtain a larger sample of $D^+ \to \pi^+\pi^+\pi^-$ decays.

New upper limits have been obtained in two regions of dimuon mass (see Figure 2 and Table 1) and the total short distance BF is extrapolated assuming a phase space model. The limits on the total BFs are $BF(D^+_s \to \pi^+\mu^+\mu^-) < 7.3 \times 10^{-8}$ (90% CL) and $BF(D^+_s \to \pi^+\mu^+\mu^-) < 4.1 \times 10^{-7}$ (90% CL) [16].

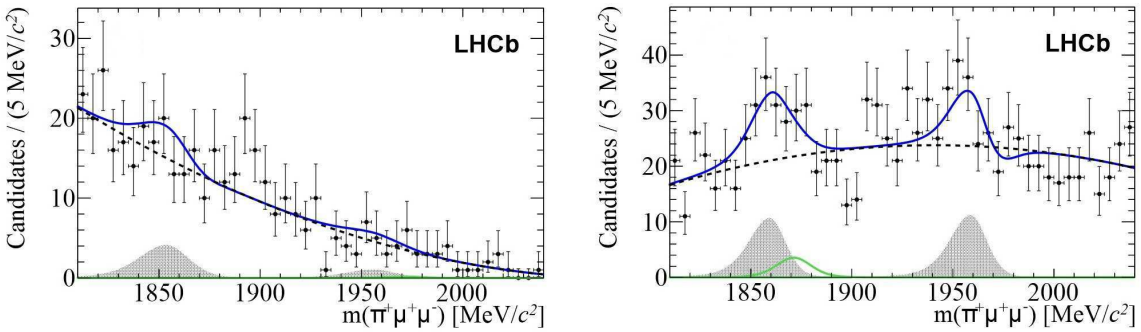

Figure 2: Invariant mass distributions for $D^+_{(s)} \to \pi^+\mu^+\mu^-$ [16] candidates in two dimuon invariant mass regions: the low-$\mu^+\mu^-$ (on the left) and high-$\mu^+\mu^-$ (on the right). The data are shown as points (black) and the total PDF (blue line) is overlaid. The components of the fit are also shown: the signal (green line), the peaking background (solid area) and the non-peaking background (dashed line).

Lepton number violating processes such as $D^+_{(s)} \to \pi^-\mu^+\mu^+$ are forbidden in the SM. The previous best upper limits are $BF(D^+ \to \pi^-\mu^+\mu^+) < 2.0 \times 10^{-6}$ and $BF(D^+_s \to \pi^-\mu^+\mu^+) < 1.4 \times 10^{-5}$ at 90% CL [17]. New searches are performed in four regions of mass $m(\mu^+\pi^-)$, in order to be more sensitive to a potential Majorana neutrino in the region where its mass may lie. Upper limits are presented in Table 2. The total upper limits are extrapolated with the same assumption as above and are equal $BF(D^+ \to \pi^-\mu^+\mu^+) < 2.2 \times 10^{-8}$ and $BF(D^+_s \to \pi^-\mu^+\mu^+) < 1.2 \times 10^{-7}$ at 90% CL [16].

These upper limits are almost 50 times better than the previous ones but they are still orders of magnitude above the SM predictions and BF enhancements from possible NP are not excluded yet.

	$m(\mu^+\mu^-)$ region, [MeV/c^2]	
Decay mode	250 - 525	1250 - 2000
$D^+ \to \pi^+\mu^+\mu^-$	2.0 (2.5) $\times 10^{-8}$	2.6 (2.9) $\times 10^{-8}$
$D^+_s \to \pi^+\mu^+\mu^-$	6.9 (7.7)$\times 10^{-8}$	16.0 (18.6)$\times 10^{-8}$

Table 1: Upper limits at the 90% (95%) CL on the branching fractions for FCNC $D^+_{(s)} \to \pi^+\mu^+\mu^-$ decays in the regions of dimuon mass sensitive to the short distance contributions.

	$m(\mu^+\pi^-)$ region, [MeV/c^2]			
Decay mode	250 - 1140	1140 - 1340	1340 - 1540	1540 - 2000
$D^+ \to \pi^-\mu^+\mu^+$	1.4 (1.7) $\times 10^{-8}$	1.1 (1.3)$\times 10^{-8}$	1.3 (1.5)$\times 10^{-8}$	1.3 (1.5)$\times 10^{-8}$
$D^+_s \to \pi^-\mu^+\mu^+$	6.2 (7.6)$\times 10^{-8}$	4.4 (5.3)$\times 10^{-8}$	6.0 (7.3)$\times 10^{-8}$	7.5 (8.7)$\times 10^{-8}$

Table 2: Upper limits at the 90% (95%) CL on the branching fractions for LNV $D^+_{(s)} \to \pi^-\mu^+\mu^+$ decays in four regions of hypothetical Majorana neutrino mass $m(\mu^+\pi^-)$.

4. Conclusions

Rare charm decays are powerful tools for the search of physics beyond the Standard Model. Their searches are an important part of LHCb's physics program. The presented results are based on 1.0 fb^{-1} of data collected in 2011. The measured upper limits still lie above the SM expectations.

References

[1] I.I. Bigi, A. Paul, *On CP Asymmetries in Two-, Three- and Four-Body D Decays*, *JHEP* **03** (2012) 021 [hep-ph/11102862].

[2] S. Fajfer, N. Kosnik, *Resonance catalyzed CP asymmetries in $D \to Pl^+l^-$*, *Phys. Rev. D* **87** (2013) 054026 [hep-ph/12080759].

[3] L. Cappiello, O. Cata, G. D'Ambrosio, *Standard Model prediction and new physics tests for $D^0 \to h^+h^-l^+l^-$ ($h = \pi, K$; $l = e, \mu$)*, [hep-ph/12094235].

[4] R. Aaij et al. (LHCb collaboration), *Prompt charm production in pp collisions at $\sqrt{s} = 7$ TeV*, *LHCb-CONF-2010-013*.

[5] A. A. Alves Jr. et al. (LHCb collaboration), *The LHCb detector at the LHC*, *JINST* **3** (2008) S08005.

[6] R. Aaij et al. (LHCb collaboration), *The LHCb trigger and its performance in 2011*, *JINST* **8** (2013) 04022 [hep-ex/12113055].

[7] A. L. Read, *Presentation of search results: The CL(s) technique*, *J. Phys. G* **28** (2002) 2693.

[8] G. Burdman et al., *Rare Charm Decays in the Standard Model and Beyond*, *Phys. Rev. D* **66** (2002) 014009 [hep-ph/0112235].

[9] E. Golowich et al., *Relating D0-anti-D0 Mixing and D0->l+l- with New Physics*, *Phys. Rev. D* **79** (2009) 114030 [hep-ph/09032830].

[10] M. Petric, M. Staric, for the Belle collaboration, *Search for leptonic decays of D0 mesons*, *Phys. Rev. D* **81** (2010) 091102 [hep-ex/10032345].

[11] R. Aaij et al. (LHCb collaboration), *Search for the rare decay $D^0 \to \mu^+\mu^-$*, *LHCb-PAPER-2013-013* [hep-ex/13055059].

[12] G. Buchalla et al., *B, D and K decays*, *Eur. Phys. J. C* **57** (2008) 309;
S. Fajfer, S. Prelovsek, P. Singer, *Rare charm meson decays $D \to Pl^+l^-$ and $c \to ul^+l^-$ in SM and MSSM*, *Phys. Rev. D* **64** (2001) 114009 [hep-ph/0106333].
A. Paul, I. I. Bigi, and S. Recksiegel, *On $D \to X_u l^+ l^-$ within the Standard Model and frameworks like the littlest Higgs model with T parity*, *Phys. Rev. D* **83** (2011) 114006 [hep-ph/11016053].

[13] S. Fajfer, N. Kosnik, S. Prelovsek, *Updated constraints on new physics in rare charm decays*, *Phys. Rev. D* **76** (2007) 074010 [hep-ph/07061133].

[14] V. Abazov et al. (D0 collaboration), *Search for flavor-changing-neutral-current D meson decays*, *Phys. Rev. Lett.* **100** (2008) 101801 [hep-ph/07082094].

[15] J. Link et al. (FOCUS collaboration), *Search for rare and forbidden three body dimuon decays of the charmed mesons D^+ and D_s^+*, *Phys. Lett. B* **572** (2003) 21 [hep-ex/0306049].

[16] J. Lees et al. (BaBar collaboration), *Search for $D^+_{(s)} \to \pi^+\mu^+\mu^-$ and $D^+_{(s)} \to \pi^-\mu^+\mu^+$ decays*, *Phys. Lett. B* **724** (2013) 203212 [hep-ex/13046365].

[17] J. Lees et al. (BaBar collaboration), *Searches for rare or forbidden semileptonic charm decays*, *Phys. Rev. D* **84** (2011) 072006 [hep-ex/11074465].